J. Fluid Mech. (2011), *vol.* 670, *pp.* 66–84. © Cambridge University Press 2011
doi:10.1017/S0022112010005392

The formation and evolution of stratification during transient mixing ventilation

ANDREA S. KUESTERS AND ANDREW W. WOODS†

BP Institute, University of Cambridge, Cambridge CB3 OEZ, UK

(Received 26 April 2010; revised 17 September 2010; accepted 29 September 2010;
first published online 31 January 2011)

We investigate the buoyancy-driven ventilation of an enclosed volume of buoyant fluid, which is connected to the exterior through two openings at the top of the enclosure. An exchange flow becomes established, with outflow through one opening being matched by an equal and opposite inflow through the other vent. The inflowing flux of dense exterior fluid develops a turbulent buoyant plume, which mixes with the interior fluid as it cascades to the base of the fluid volume. An upward return flow gradually stratifies the confined volume of fluid, with a first front of relatively dense plume fluid advancing to the top of the space. Initially, the exchange flow is steady, but as the first front rises above the inflow opening, the flow rate wanes. The initial development of the exchange flow and interior stratification follows the classical filling box work of Baines & Turner (*J. Fluid Mech.*, vol. 37, 1969, p. 51), with a plume of constant buoyancy flux. Once the first front exits the space, the volume flux rapidly asymptotes to the form $Q = Q_0(\tau/(\tau + t))$ from the initial value Q_0, where τ is the buoyancy-driven draining time, based on the initial density contrast with the environment. The vertical structure of the interior density stratification asymptotes to a profile of constant shape whose amplitude decays in time as $(\tau/(\tau + t))^2$, and we identify conditions under which the vertical variation in density is comparable to the difference between mean interior density and the exterior. This generalises the analysis presented by Linden, Lane-Serff & Smeed (*J. Fluid Mech.*, vol. 212, 1990, p. 309), who assumed that the interior fluid is well mixed. New laboratory experiments of the process are shown to be consistent with our predictions of the evolution of the flow, the interior stratification and the migration of contaminants. We also develop our analysis for situations where there are multiple stacks and show how this improves the mixing efficiency for a given ventilation flow. The model has relevance for the design of transient mixing ventilation in a building, especially when the effect of vertical stratification is important for ensuring thermal comfort.

Key words: Plumes/thermals

1. Introduction

There are numerous examples in which buoyant fluid in a confined space exchanges with fluid in the exterior through an opening, or series of openings, in the walls of the container (figure 1). Important examples include the exchange of internal hot air and external cold air through high-level openings in a building (Linden *et al.* 1990; Boulard & Baille 1995; Linden 1999; Chiu & Etheridge 2004; Chenvidyakarn &

† Email address for correspondence: andy@bpi.cam.ac.uk

https://doi.org/10.1017/S0022112010005392 Published online by Cambridge University Press

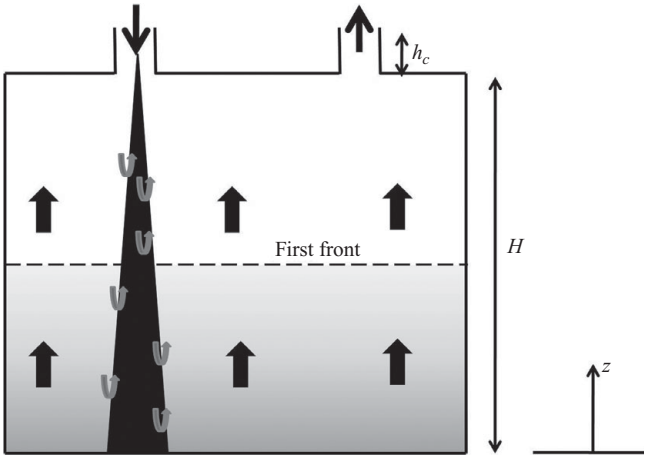


FIGURE 1. Set-up of the room with two roof vents. Illustration of the buoyancy-driven draining and mixing flow regime during the early time when the first front is still within the enclosed space.

Woods 2005; Fitzgerald & Woods 2008; Liu, Lin & Chou 2009; Woods, Fitzgerald & Livermore 2009), the flushing of smoke from a building through vents (Merci & Maele 2008), and the exchange of saline and fresh fluid over a sill, which connects relatively saline and fresh water masses in the ocean (Pawlak & Armi 2000; Wells & Wettlaufer 2007). The flow involves outflow of relatively light fluid and an equal inflow of relatively dense fluid. If the inflow has sufficient flux, it will form a turbulent buoyant plume as it descends through the confined layer of fluid. The entrainment of the ambient fluid into this plume leads to mixing of the interior fluid and formation of stratification as in the classical model of Baines & Turner (1969) (figure 1). However, once the so-called first front of mixed ambient and plume fluid passes the inflow vent, the buoyancy contrast driving the flow decreases; eventually, the first front reaches the outflow vent and the whole interior space becomes stratified. The continued inflow of dense exterior fluid continually reduces the buoyancy of the interior fluid, and so the overall flow wanes, while the interior fluid becomes progressively denser. The purpose of this paper is to explore this transient ventilation flow. We develop a mathematical model for the rate of draining of the buoyant fluid, for the evolution of the density both with depth and with time inside the space, and for the rate of migration of a front of contaminants through the space. We first consider a space with two roof-level vents (figure 1) in §§ 2–4 and then investigate the flow when there are multiple stacks in § 5.

The problem is of especial interest for the natural ventilation of buildings in colder conditions when mixing ventilation may often be the preferred mode of ventilation. Indeed, if the external temperature is colder than the internal comfort temperature of the occupants, then the incoming ventilation air requires some pre-heating prior to contact with the occupants. In natural ventilation, one can either use upward displacement ventilation, in which the incoming air at low level requires some mechanical pre-heating or mechanical mixing with the interior air, or one can use mixing ventilation in which the incoming air enters at high level, and mixes by natural convection with the interior air, prior to reaching the occupants. This latter regime of flow may be applied in theatres or other high spaces, such as atria. There may be substantial energy savings associated with such natural mixing ventilation, especially in buildings for which the internal heat gains exceed the heat losses, as is

https://doi.org/10.1017/S0022112010005392 Published online by Cambridge University Press

often the case in modern well-insulated buildings when the exterior temperature lies above values of order 5–10 °C (Woods *et al.* 2009). By assuming that the space is well mixed, they showed that savings of well over 50 % of the energy required for the pre-heating of winter ventilation air is possible. Also, in summer, naturally ventilated buildings often adopt a strategy of night-cooling, in order to remove some of the diurnal heat gains while the exterior temperature is relatively low. Again, mixing ventilation may be an ideal means to night-cool the building; it reduces the risks that very cold night-time air can overcool the building since the incoming air is pre-heated through mixing.

When adopting natural mixing ventilation, there are often situations in which transient ventilation is adopted to allow the building to cool through a natural exchange flow at high level in the building. The transient cooling associated with this, for example, during the interval in a theatrical performance, leads to a gradual decrease in temperature and the development of stratification in the space, as the plume of relatively cold incoming air descends and mixes. This problem is of especial interest herein and forms the main topic of this paper. Although Linden *et al.* (1990) explored a simplified well-mixed model of this transient flow, there are situations in which the interior stratification which develops is very significant. This is important as it leads to different temperatures at different heights and hence the possibility for thermal discomfort. We also present new experiments to illustrate how contaminants may be transported by such a transient flow during mixing ventilation with the important recognition that a localised region of concentrated contaminant largely remains localised as it migrated through the stratified space, rather than being immediately well mixed throughout the flow.

In developing the models, we draw on previous work which has examined the transient evolution of density in a confined space with turbulent buoyant plumes and return flow in the ambient fluid (Baines & Turner 1969; Germeles 1975) and some of the modelling concepts associated with transient natural ventilation (Kaye & Hunt 2004; Bolster & Linden 2007; Bolster, Maillard & Linden 2008; Bower *et al.* 2008; Flynn & Caulfield 2006). In their pioneering work, Linden *et al.* (1990) presented some experiments of the flow configuration shown in figure 1, but their analysis focused on the well-mixed case. The present analysis and new experiments provide more information and quantitative understanding of the flow and stratification of density within the space. In particular, we recognise that, at long time, the density evolves according to a simple function of time, with the vertical density stratification being given by a fixed shape whose amplitude decays with time. We also note that Caulfield & Woods (2002) presented a study somewhat related to the present paper in which a constant flux of fluid of fixed density was supplied to an enclosed space, with a constant outflow flux at the same level as the inflow so that the interior density gradually evolves to that of the supply fluid. A key difference with the present work on natural draining flows is that here the ventilation rate evolves with the density and this leads to a different evolution of buoyancy of the space. We also support our analysis with a series of new laboratory experiments which identify the spatial and time-dependent evolution of the mixing, and we extend the analysis to account for the possibility of multiple openings on the roof.

2. Model for buoyancy-driven draining in a room with two roof-level vents

Our model is based on the exchange flow through two openings at the top of the space (figure 1), each of area A_c and height h_c, with buoyant fluid leaving through

https://doi.org/10.1017/S0022112010005392 Published online by Cambridge University Press

one opening and an equal amount of exterior fluid entering through the other vent. Throughout this paper, we assume that there is a uni-directional flow through each opening. This assumption is appropriate in the case that the chimney height, h_c, exceeds the radius of the chimney, $\sqrt{A_c/\pi}$. For $h_c \approx \sqrt{A_c/\pi}$, the flow may become unstable with intermittent periods involving an exchange flow in each opening or a uni-directional flow in each opening (Kenton *et al.* 2004); however, in this paper, we focus on the case of unidirectional flows.

Prior to developing a full model of the evolution of the interior density and associated stratification, it is useful to consider the simplified situation in which the interior remains well-mixed at all times.

2.1. *A well-mixed model*

Our analysis of the well-mixed model follows that of Linden *et al.* (1990); we use this model as a reference to illustrate the efficiency of the mixing associated with the incoming plume. We assume that the space is well-mixed, and buoyant fluid of density $\rho_0 - \Delta\rho_{wm}(t)$ is venting from the space and fluid of density ρ_0 is entering the space. If the two openings have the form of chimneys, of height h_c, then the volume flux in each direction, πQ_e, is given by

$$\pi Q_{wm}(t) = cA_c \left(\frac{g h_c \Delta\rho_{wm}(t)}{\rho_0} \right)^{1/2}, \tag{2.1}$$

where c is an effective loss coefficient and g is the acceleration due to gravity. The buoyancy flux venting from the space causes the buoyancy of the space of volume V to evolve according to the relation

$$\frac{\mathrm{d}\Delta\rho_{wm}(t)}{\mathrm{d}t} = -\frac{cA_c \Delta\rho_{wm}(t)^{3/2}}{V} \left(\frac{g h_c}{\rho_0} \right)^{1/2}, \tag{2.2}$$

with solution

$$\frac{\Delta\rho_{wm}(t)}{\Delta\rho_{wm}(0)} = \left(\frac{\tau}{\tau + t} \right)^2, \tag{2.3}$$

where

$$\tau = \frac{2V}{cA_c} \left(\frac{\rho_0}{\Delta\rho_{wm}(0) g h_c} \right)^{1/2}, \tag{2.4}$$

(cf. (3.3*a*) and (3.3*b*) in Linden *et al.* 1990). In the remainder of this section, we examine the case in which the mixing is driven by the turbulent buoyant plume produced by the inflow of the external fluid. We show that after the exit of the first 'filling box' front (cf. Baines & Turner 1969), the density stratification continually adjusts so that the mean density decays according to a law similar to (2.3). We also present some new experimental results which we compare with the model predictions.

2.2. *The numerical model for buoyancy-driven draining*

We assume that the inflowing fluid enters an enclosed region of fluid, of volume V, at height $z = H$, with the fluid located in the region $0 < z < H$, and the space has a constant cross-sectional area $A = V/H$. The volume flux through the roof vent is

$$\pi Q_e = cA_c \left(\frac{g h_c \Delta\rho(H, t)}{\rho_0} \right)^{1/2}, \tag{2.5}$$

where $\rho_e(z, t) = \rho_0 - \Delta\rho(z, t)$ is the interior density as a function of time t and space z (cf. (2.1)). We assume that the inflowing fluid forms a turbulent buoyant plume

https://doi.org/10.1017/S0022112010005392 Published online by Cambridge University Press

with volume flux $\pi Q(z,t)$, momentum flux $\pi M(z,t)$ and buoyancy flux $\pi F(z,t)$ (cf. Morton, Taylor & Turner 1956), which follow the equations for a quasi-steady descending turbulent buoyant plume (moving from $z=H$ to $z=0$):

$$\frac{\partial Q}{\partial z} = -2\alpha M^{1/2}, \tag{2.6a}$$

$$M\frac{\partial M}{\partial z} = -FQ, \tag{2.6b}$$

$$\frac{\partial F}{\partial z} = \left(\frac{g}{\rho_0}\frac{\partial \rho_e}{\partial z}\right) Q, \tag{2.6c}$$

where α is a turbulent entrainment coefficient, with value 0.12 ± 0.01 (Turner 1979). We assume that the plume has a top hat profile. Following Baines & Turner (1969), the ambient density evolves according to the advection equation

$$\frac{\partial \rho_e}{\partial t} = -\frac{\pi Q}{A}\frac{\partial \rho_e}{\partial z}, \tag{2.7}$$

in the region below the first front, which is composed of the first plume fluid to reach the base of the enclosure and subsequently to be advected back up through the ambient fluid towards the top of the enclosure. In the region above the first front, the ambient density equals the initial density in the enclosure, and so up to the point when the first front reaches the top of the enclosure, the fluid venting from the space also equals the initial density in the enclosure. During this period, the plume has constant source buoyancy flux

$$F_0 = g\Delta\rho_0 Q_0/\rho_0, \tag{2.8}$$

where πQ_0 and $\Delta\rho_0$ are the initial volume flux ((2.5) at $t=0$) and density contrast between the interior and exterior flux, respectively. The time scale required for the filling front to vent from the room is given by the filling box time, τ_f, which scales with the room volume divided by the volume flux of the plume at the base of the room. The volume flux of the plume scales with the source buoyancy flux and the height of the room according to the relation $Q \approx \lambda F_0^{5/3} H^{5/3}$, where $\lambda = 6/5\left((9/10)\pi^2\right)^{1/3}\alpha^{4/3}$. Using the empirical value $\alpha = 0.12$, we find that $\lambda \approx 0.15$ (Morton *et al.* 1956), and so the filling box time scales as (see Baines & Turner 1969)

$$\tau_f = \frac{3A}{2\lambda F_0^{1/3} H^{2/3}}. \tag{2.9}$$

Comparison with the draining time τ (see (2.4)) shows that in the present problem, the filling box time is related to the draining time by a geometrical factor (Kaye & Hunt 2004):

$$\tau_f = \left(\frac{3h_c^{1/3}\pi^{1/3}(cA_c)^{2/3}}{4\lambda H^{5/3}}\right)\tau = \left(\frac{3\pi^{1/3}}{4\lambda}\left(\frac{(cA_c)}{H^2}\sqrt{\frac{h_c}{H}}\right)^{2/3}\right)\tau. \tag{2.10}$$

Note that cA_c/H^2 is the factor as in Linden *et al.* (1990) and the additional factor of $\sqrt{h_c/H}$ accounts for the flow driven by the stacks.

In figure 2, we illustrate the variation of the ratio τ_f/τ with h_c/H for $d/H = 0.01$, where d is the radius of the inflow opening. The figure shows that for reasonable sized stacks, the filling box time is a small fraction of the draining time, so that the

https://doi.org/10.1017/S0022112010005392 Published online by Cambridge University Press

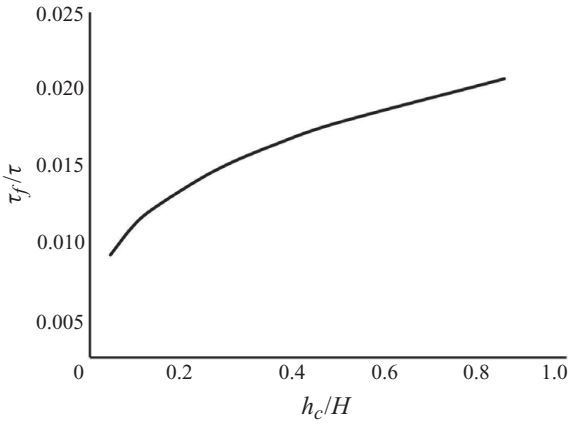


FIGURE 2. The ratio of the filling box time and the draining time, τ_f/τ, as a function of h_c/H for $d/H = 0.01$.

main part of the flow occurs once the first front has vented from the space. We now focus on this long-time draining flow.

Once the first front reaches the outflow vent, the outflowing fluid becomes progressively more dense, and, as a result, the rate of draining wanes. To study this flow, we have solved the governing equations (2.6) and (2.7) numerically using the boundary conditions that (i) the inflow exchange flux is given by (2.5), with $\Delta\rho$ evaluated at the height of the outflow; (ii) at the base of the enclosure, the plume buoyancy equals that of the ambient so that $F = 0$ at $z = 0$; and (iii) the momentum flux of the inflowing plume is related to the volume flux according to the relation

$$M = \frac{Q^2}{d^2}, \tag{2.11}$$

at $z = H$. The numerical approach follows the method described by Germeles (1975), in which density surfaces in the ambient fluid are repeatedly advected through space over a fixed time step, thereby leading to a spatially evolving grid of constant-density surfaces. Figure 3 illustrates the dimensionless buoyancy profile as a function of dimensionless height and time,

$$y = z/H, \tag{2.12a}$$

$$s = t/\tau, \tag{2.12b}$$

where τ is the draining time given in (2.4),

$$b(y, s) = \delta\rho(y, s)/\delta\rho(1, 0), \tag{2.13}$$

where

$$\delta\rho(y, s) = \rho_e(y, s) - \rho_0, \tag{2.14}$$

with ρ_0 being the exterior density.

In figure 4, we show the evolution of the ventilation flux as a function of dimensionless time (figure 4*a*), and the mean buoyancy (figure 4*b*) as defined by the relation

$$\bar{b}(s) = \int_0^1 b(y, s)\,\mathrm{d}y. \tag{2.15}$$

https://doi.org/10.1017/S0022112010005392 Published online by Cambridge University Press

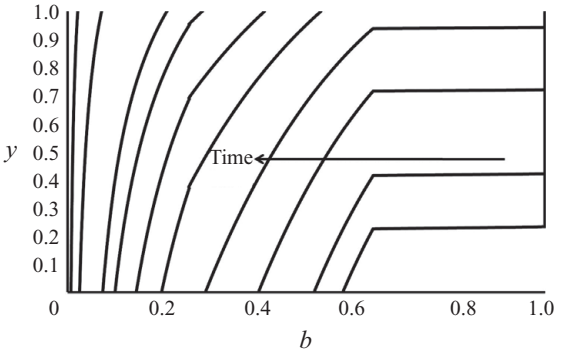


FIGURE 3. Evolution of the density profiles with time as a perfect plume reaches the base of the tank and forms a stratified layer. $d/H = 0.16$. Curves are shown at the dimensionless times $s = 0.04$, 0.09, 0.18, 0.27, 0.40, 0.53, 0.71, 0.88, 1.77, 3.54 (from right to left).

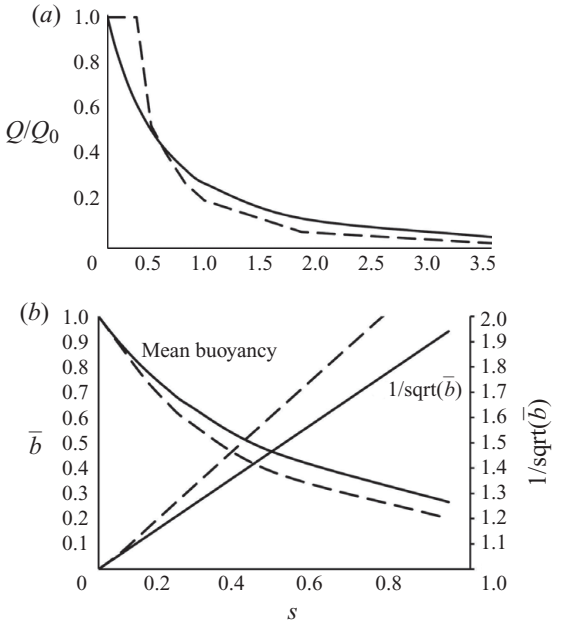


FIGURE 4. Comparison of (*a*) the evolution of the ventilation rate as a function of dimensionless time and (*b*) both the variation of the mean buoyancy in the space as a function of dimensionless time and also the variation of $1/\mathrm{sqrt}(\bar{b})$ on the second axis. We are comparing the full numerical solution from § 2.2 for a perfect plume (dashed lines) with the well-mixed model from § 2.1 (solid lines). $d/H = 0.16$.

This is compared with the predictions of the well-mixed model (see (2.1)–(2.4); solid lines). The comparison shows that soon after the first front leaves the enclosure, the ventilation rate decreases and then evolves at a rate very similar to the well-mixed regime, while the mean density in the space also evolves at a rate similar to the well-mixed model. Indeed, in figure 4(*b*), we have also plotted $1/\bar{b}(s)^{1/2}$ as a function of dimensionless time s, illustrating that this evolves linearly with time, in accord with the prediction of the well-mixed model equation (2.3).

https://doi.org/10.1017/S0022112010005392 Published online by Cambridge University Press

2.3. *Separable solution and the rate of waning of the density field*

Guided by these numerical predictions, and in particular figure 4(*b*), we expect that the ambient density profile asymptotes to a separable regime in which the density profile establishes a steady shape whose amplitude varies in time. To this end, we seek solutions of the form

$$Q(y,s) = F_0^{1/3} H^{5/3} f_q(s) q(y), \tag{2.16a}$$

$$M(y,s) = F_0^{2/3} H^{4/3} f_m(s) m(y), \tag{2.16b}$$

$$F(y,s) = F_0 f_b(s) f(y), \tag{2.16c}$$

$$b(y,s) = f_\Delta(s) \Delta(y), \tag{2.16d}$$

in terms of dimensionless functions of vertical position y and time s, and in which the reference buoyancy flux is given by

$$F_0 = \frac{g\delta\rho(1,0)}{\rho_e} Q_0, \tag{2.17}$$

with πQ_0 being the initial volume flow rate from the roof vent (see (2.5)). On substitution into the governing equations, we find that the dimensionless time functions are related according to

$$f_q(s) = \sqrt{f_\Delta(s)}, \tag{2.18a}$$

$$f_m(s) = f_q^2(s), \tag{2.18b}$$

$$f_b(s) = f_q^3(s), \tag{2.18c}$$

$$\frac{\mathrm{d}f_\Delta(s)}{\mathrm{d}s} = -2\omega f_\Delta^{3/2}(s), \tag{2.18d}$$

where ω is a dimensionless constant which determines the rate of decay of the density field, and we set

$$f_q(0) = f_m(0) = f_b(0) = f_\Delta(0) = 1. \tag{2.19}$$

We have chosen the factor 2 in (2.18*d*) so that it leads to the solution

$$f_\Delta(s) = \left(\frac{1}{\omega s + 1}\right)^2, \tag{2.20}$$

which is directly analogous to (2.3) except for the rescaling by ω. This result illustrates the agreement between the numerical solution and the well-mixed model shown in figure 4(*b*). The number ω (>1) represents the fractional reduction in the time scale for draining of buoyancy from the space, compared to the well-mixed situation. This results from there being a density gradient within the space, which leads to the fluid at the top of the space being more buoyant than the mean. We find ω by solving the equations for the spatial profile of the buoyancy, $\Delta(y)$, given by the solution of the

https://doi.org/10.1017/S0022112010005392 Published online by Cambridge University Press

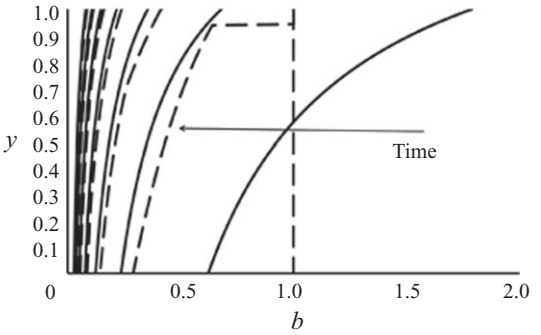


FIGURE 5. Comparison of the numerical density profiles (dashed lines) as a function of time and the density profile associated with the separable solution (solid lines) for $\hat{\Gamma} = 1.6$, $\hat{\Gamma} P = 0.25$. Profiles taken at $s = 0$, 0.27, 0.53, 0.80, 1.06, 1.33, 1.59.

ordinary differential equations

$$\frac{\mathrm{d}q}{\mathrm{d}y} = -2\alpha m^{1/2}, \tag{2.21a}$$

$$m\frac{\mathrm{d}m}{\mathrm{d}y} = -fq, \tag{2.21b}$$

$$\frac{\mathrm{d}f}{\mathrm{d}y} = \frac{\mathrm{d}\Delta}{\mathrm{d}y}\frac{q}{q(1)\Delta(1)}, \tag{2.21c}$$

$$\frac{\mathrm{d}\Delta}{\mathrm{d}y} = \frac{(\hat{\Gamma}P)^{5/3}\omega\Delta}{q}, \tag{2.21d}$$

where

$$P = d/H, \tag{2.22a}$$

$$\hat{\Gamma} = \left(\frac{F_0 d^5}{Q_0^3}\right)^{-1/5}, \tag{2.22b}$$

subject to the boundary conditions

$$\int_0^1 \Delta(y)\,\mathrm{d}y = 1, \tag{2.23a}$$

$$q(1) = (\hat{\Gamma}P)^{5/3}, \tag{2.23b}$$

$$m(1) = \hat{\Gamma}^{10/3}P^{4/3}, \tag{2.23c}$$

$$f(1) = 1, \tag{2.23d}$$

$$f(0) = 0. \tag{2.23e}$$

The latter condition ensures that the ambient density at the base of the enclosure equals the density of the plume at the base. In solving (2.21) subject to the boundary conditions (2.23), the value of ω arises as an eigenvalue. It is found by numerical shooting, integrating from $y = 1$ to $y = 0$ and selecting that value of ω for which (2.23*e*) is satisfied.

In figure 5, we compare the predictions of (2.21) and (2.23) with the solutions of the full numerical model (§2.2) in the case of $\hat{\Gamma} = 1.6$, $\hat{\Gamma} P = 0.25$. In calculating

https://doi.org/10.1017/S0022112010005392 Published online by Cambridge University Press

the separable solution, we started at dimensionless time $s = 0$ and ensured that the average density in the separable solution equals the average density in the full numerical solution at $s = 0$. There is an initial difference in the solution, owing to the adjustment of the full numerical solution from the early time steady draining regime to the separable draining regime once the first front has vented from the space. However, at longer times, the separable model provides a very accurate description of the draining (figure 5).

3. Experimental models

In order to test this model of buoyancy-driven mixing during draining, we have carried out a series of salt bath experiments using a very simple apparatus, which consisted of a tank of dimension 39.5 cm × 39.5 cm × 23 cm. Two holes were cut into the roof of the tank, each housing a stack, of radius 5.1 mm and heights of 40, 60 or 80 mm. The tank was then inverted, with rubber bungs placed at the end of each tube, and immersed in a large reservoir of fresh water, suspended well above the base of the reservoir and filled with an aqueous saline solution. The experiments were run in this inverted fashion, compared to the cartoon in figure 1, with fresh water entering the tank from below and the saline water in the tank draining out of the tank. Before the experiment commenced, a conductivity probe was immersed into the experimental tank, through a small opening in the upper surface of the tank (opposite to the face with the stacks). A small pipe was placed in this hole, the end of which was proud of the water surface in the main reservoir, to prevent ingress of fresh reservoir water at the top of the tank. Regular vertical traverses of the conductivity were then taken during the experiment, and these were converted to salinity through a series of controlled calibration experiments.

In order to find the coefficient of friction through the stacks, we evaluated the volume flux between successive profiles in the experiment during the initial phase of the rising front and compared this with the theoretical prediction, i.e. (2.5). For a more complete analysis of friction in the stacks and pressure loss as a result of this, see Livermore & Woods (2006).

Following removal of the two bungs at the end of the stacks, an exchange flow between the enclosed space and the large reservoir was established. Figure 6 illustrates the typical evolution of the fluid in the enclosed space, showing four images at successive times during an experiment. The plume fluid is initially dyed green and then red in order to help visualise the stratification and descent of the density fronts. Numerous near horizontal surfaces can be seen in the photographs associated with internal waves in the stratified fluid. During the experiment, we found that once the flow direction through the stacks is established, the direction does not change.

The experiment was carried out several times in order to ensure repeatability. Figures 7(*a*)–7(*c*) compare the measured density profiles (dashed lines) with the model predictions (dotted lines) for three experiments using stack heights of 40, 60 and 80 mm. In each case, the initial salinity of the fluid was 20 %. Figure 7(*d*) shows an experiment in which the aqueous solution was 15 % weight with a stack height of 80 mm. Over the duration of each experiment, there is reasonable agreement between the density profiles from the experiments and the theoretical prediction.

As a further mean of testing our theoretical prediction, we considered the evolution of fronts of constant density. Theoretically, for a plume starting at $z = H$ and

https://doi.org/10.1017/S0022112010005392 Published online by Cambridge University Press

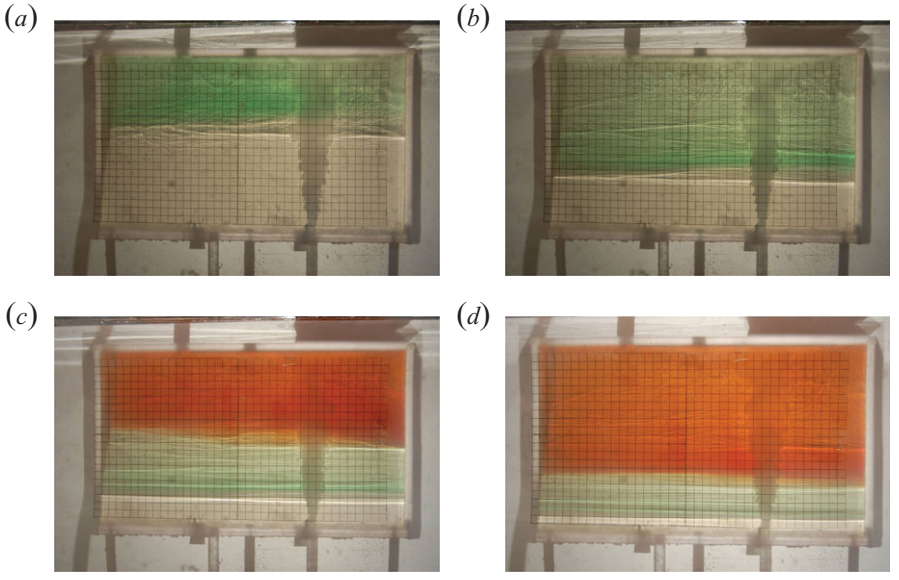


FIGURE 6. (Colour online at journals.cambridge.org/FLM) Sequence of images of the evolution of the flow in the experimental model. In this model, fresh water enters the reservoir from below into the experimental tank, and the dense fluid vents from a second opening on the base of the tank. The input fluid is dyed a successive series of colours to help track the filling fronts. Each photograph was taken 90 s after the preceding picture.

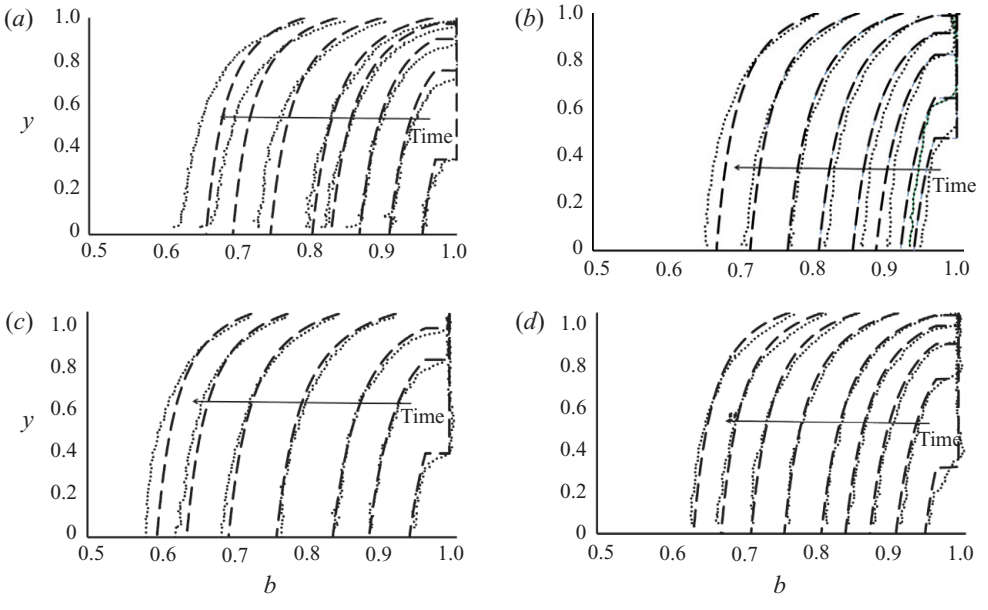


FIGURE 7. The evolution of the buoyancy distribution of the fluid within the enclosed space comparing the experimental data (dotted lines) and theoretical model (dashed lines). (*a*) Stack height: 40 mm; initial salinity: 20 %. (*b*) Stack height: 60 mm; initial salinity: 20 %. (*c*) Stack height: 80 mm; initial salinity: 20 %. (*d*) Stack height: 80 mm; initial salinity: 15 %.

https://doi.org/10.1017/S0022112010005392 Published online by Cambridge University Press

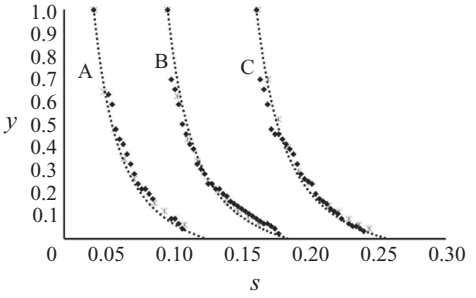


FIGURE 8. The descending front as obtained from photographs (diamonds) from the profiles (stars) and the theoretical prediction (dots) near the start of the experiment, $s = 0.02$ (curve A), just before the transition from the filling box front, $s = 0.08$ (curve B), and during the long-time evolution, $s = 0.15$ (curve C). For reference, the first front exits the space at $s = 0.09$. $h_c = 80$ mm.

descending to the bottom, the height of the front, $z_f = Hy_f$, is given by

$$\frac{\mathrm{d}z_f}{\mathrm{d}t} = \frac{Q(z_f, t)}{A}, \tag{3.1}$$

where, using (2.16*a*),

$$Q(z_f, t) = F_0^{1/3} H^{5/3} q(z_f/H) \left(\frac{1}{\omega t/\tau + 1}\right), \tag{3.2}$$

and, in this expression, the solution of $q(z_f/H)$ is numerically given by solving (2.21)–(2.23). It follows using dimensionless parameters that the height of the front, y_f, is implicitly given by

$$\int_0^{y_f} \frac{1}{q(y)}\,\mathrm{d}y = \frac{2}{\omega(\hat{\Gamma}P)^{5/3}} \ln(\omega s + 1). \tag{3.3}$$

From the experiment, there are two ways of obtaining the evolving front: (i) by dying the incoming plume and taking photographs at constant intervals showing the descent of the front and (ii) by looking at the surfaces of constant density in the experimental profiles obtained from the conductivity probe. Figure 8 shows the height of the leading edge of a dye front (diamonds) and position of the salinity surfaces (stars) as a function of time. Three sets of data are shown, corresponding to dye release near the start of the experiment (curve A), just before the transition from the initial phase to the long-time regime (curve B) and in the long-time separable regime (curve C). The two sets of data agree well as expected since the dye and the salinity fields track each other. As can be seen, the agreement between the data and the theoretical prediction is also very good. There is a small offset due to the sloshing of the plume at the ceiling but otherwise our theory from § 2.2 is accurate, and thus, the volume flux through the stacks and the plume behaviour in the space is consistent with the predictions of the model. Furthermore, this again illustrates that the system is not well mixed, and the development and evolution of the stratification are important for tracking the contaminant as well as predicting the magnitude of the temperature gradient in the space.

https://doi.org/10.1017/S0022112010005392 Published online by Cambridge University Press

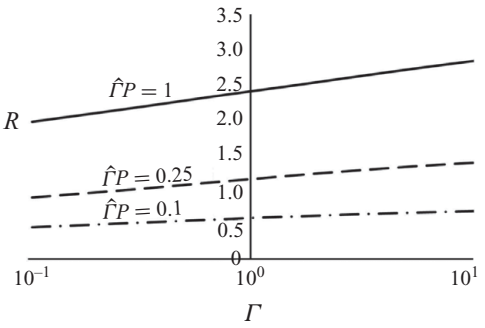


FIGURE 9. $R = (b(1) - b(0))/\bar{b}$ as a function of Γ for $\hat{\Gamma}P = 0.1$ (dashed–dotted line), 0.25 (dashed line) and 1 (solid line).

4. Mixing efficiencies

In the context of natural ventilation, understanding the magnitude of the stratification is critical for ensuring thermal comfort throughout the space. The analysis and experiments above reveal that significant vertical stratification can develop. For example, if the difference in density of the high- and low-level fluid relative to the mean is of order 20%, then with an interior space at a mean temperature of 22 °C and exterior at 2 °C, there will be a variation in temperature in the interior from 20 to 24 °C, which may lead to the lower region of the building being too cold, while there are relatively warm temperatures higher in the space.

We therefore explore the mixing efficiency of the plume in more detail to establish flow regimes for which there is significant stratification, thereby extending the analysis of Linden *et al.* (1990), which considered only the well-mixed case. The mixing efficiency depends on the plume mixing which, in turn, depends on the geometry of the inflow opening as characterised by the stack height h_c and the radius d, since this changes the characteristics of the flow (Caulfield & Woods 1998; Hunt & Kaye 2001). In particular, we can estimate whether the flow is initially like a jet, perfect plume or distributed (lazy) plume using the source parameter

$$\Gamma = \frac{5Q_0^2F_0}{4\alpha M_0^{5/2}} = \frac{5}{4\alpha}\frac{F_0d^5}{Q_0^3} = \frac{5d}{4\alpha c^2H_c} = \frac{5}{4\alpha}\hat{\Gamma}^{-5}. \tag{4.1}$$

When the flow is in perfect plume balance, $\Gamma = 1$. If $\Gamma > 1$, the flow has a deficiency of buoyancy near the source and is known as a distributed plume and, for $\Gamma < 1$, the flow is jet-like near the source. We expect the mixing to be more efficient in the case of a jet and less efficient for a distributed plume; indeed, a distributed plume may contract as it enters the space and thus entrains less ambient fluid, resulting in a somewhat greater stratification.

To confirm these expectations, in figure 9 we show how the density difference between the top and the bottom of the space relative to the mean, $R = (b(1) - b(0))/\bar{b}$ say, varies with Γ for three different values of $\hat{\Gamma}P$. R may be regarded as a dimensionless measure of the stratification. For a typical value of $\Gamma = 1$ and $P = 0.16$, $R \approx 1.15$, thus showing that the interior vertical stratification can be significant. This may be important when considering thermal comfort for the occupants, for example, during the interval at a theatre.

We now investigate the effect that such stratification has on the evolution of the average density in the space since we expect a more stratified layer to evolve more

https://doi.org/10.1017/S0022112010005392 Published online by Cambridge University Press

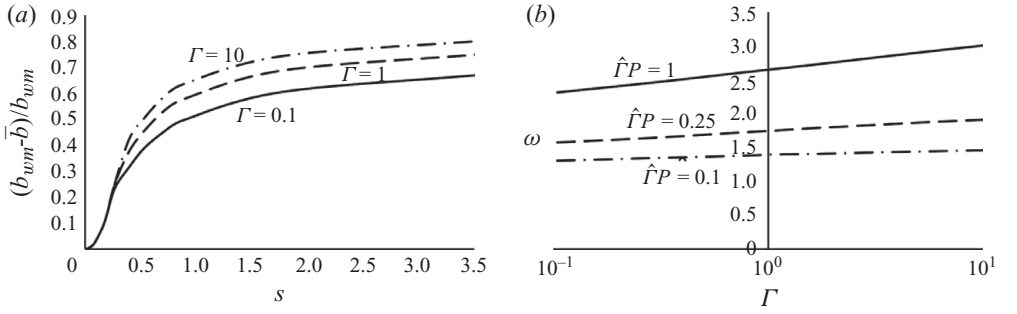


FIGURE 10. (*a*) $\hat{B} = (\bar{b} - b_{wm})/\bar{b}$ for $\Gamma = 0.1$ (solid line), $\Gamma = 1$ (dashed line) and $\Gamma = 10$ (dashed–dotted line). $\hat{\Gamma} P = 0.25$. (*b*) The eigenvalue, ω, as a function of Γ for different values of $\hat{\Gamma} P = 0.1$ (dashed–dotted line), 0.25 (dashed line) and 1 (solid line).

rapidly (cf. figure 4*b*). In order to compare the evolution, we introduce a dimensionless buoyancy difference $\hat{B} = (b_{wm} - \bar{b})/b_{wm}$, given by the difference between the buoyancy b_{wm} predicted by the well-mixed model (§ 2.1) and the mean buoyancy $\bar{b}$ as predicted by the full stratified model (§ 2.2) as a fraction of the buoyancy of the well-mixed model, b_{wm}. Figure 10(*a*) shows the variation of $\hat{B}$ with time for three different values of Γ ($\Gamma = 0.1$, 1, 10). It can be seen that the vertical density stratification leads to a more rapid evolution of the average buoyancy in the space, and this difference is larger for greater degrees of stratification, i.e. larger values of Γ. In particular, with large vertical stratification, the time evolution of the average density decreases since the density of the driving fluid is larger than the mean. The difference in this evolution is quantified by the eigenvalue ω of the separable solution (cf. (2.20)). In figure 10(*b*), we show how the eigenvalue ω varies with Γ for $\hat{\Gamma} P = 0.1$, 0.25, 1. We find that $1 < \omega < 3$.

5. Three or more stacks

Most real buildings have multiple stacks, and this can lead to a more complex evolution of the interior stratification since we expect more mixing for a given buoyancy flux if the buoyancy flux is distributed over a series of plumes (Linden & Cooper 1996). We now extend our analysis to account for the case of N equal stacks with inflow through n stacks and outflow through $N - n$ stacks. We assume that all the stacks are identical, and therefore, the inflowing plumes have the same buoyancy flux, $F_n = g\Delta\rho_0 Q_N/(n\rho_0)$, where Q_N is the total volume flux entering the space through the n stacks, which is given by

$$Q_N = cA_c^* \sqrt{\frac{g\Delta\rho(H,t)h_c}{\rho_0}}, \tag{5.1}$$

where A_c^* is the effective area of the openings. This is given by

$$A_c^* = \frac{\sqrt{2}A_{in}A_{out}}{\sqrt{A_{in}^2 + A_{out}^2}} = \frac{\sqrt{2}n(N-n)}{\sqrt{n^2 + (N-n)^2}} A_c, \tag{5.2}$$

where $A_{in} = nA_c$ is the sum of the area of the stacks with inflowing exterior fluid and $A_{out} = (N - n)A_c$ is the sum of the area of the stacks through which the space is drained. Figure 11 shows how $Q_N/(nQ)$ varies for different values of N and n. It can

https://doi.org/10.1017/S0022112010005392 Published online by Cambridge University Press

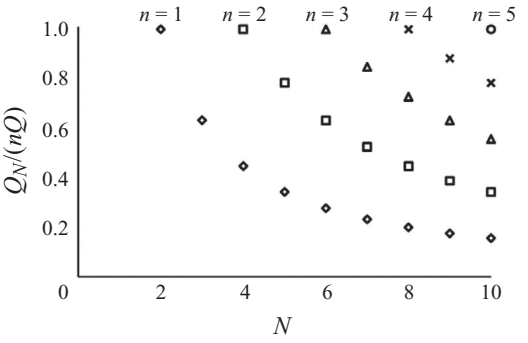


FIGURE 11. $Q_N/(nQ)$ as a function of N, for different numbers of inflowing plumes.

be seen that for an equal number of inflowing and outflowing plumes, the volume flux, Q_N, is the same as for two large openings of area nA_c and volume flux Q. As the difference between the number of inflowing and outflowing plumes increases, the volume flux decreases.

Combining (5.1) and (5.2) with the well-mixed model from § 2, we find that

$$\frac{\Delta\rho_{wm}(t)}{\Delta\rho_{wm}(0)} = \left(\frac{\tau}{\tau + t}\right)^2, \tag{5.3}$$

where

$$\tau = \frac{2V}{cA_c^*}\left(\frac{\rho_0}{\Delta\rho_{wm}(0)gh_c}\right)^{1/2}. \tag{5.4}$$

This is directly analogous to our earlier result (see (2.3) and (2.4)).

The mixing, and hence, effective entrainment produced by n plumes, each of buoyancy flux F_N/n, is greater than the mixing associated with one plume of buoyancy flux F_N. To calculate the effective mixing, we analyse the mixing associated with each incoming plume as given by the plume equations and calculate the density evolution by using the advection equation for the set of plumes. Thus, the governing set of equations for the dimensionless volume flux, q_n, momentum flux, m_n, buoyancy flux, f_n, associated with each plume and the dimensionless buoyancy in the space, Δ_N, is given by

$$\frac{\mathrm{d}q_n}{\mathrm{d}y} = -2\alpha m_n^{1/2}, \tag{5.5a}$$

$$m_n\frac{\mathrm{d}m_n}{\mathrm{d}y} = -f_n q_n, \tag{5.5b}$$

$$\frac{\mathrm{d}f_n}{\mathrm{d}y} = \frac{\mathrm{d}\Delta_N}{\mathrm{d}y}\frac{q_n}{nq_n(1)\Delta_N(1)}, \tag{5.5c}$$

$$\frac{\mathrm{d}\Delta_N}{\mathrm{d}y} = \frac{(\hat{\Gamma}P)^{5/3}\omega\Delta_N}{nq}, \tag{5.5d}$$

https://doi.org/10.1017/S0022112010005392 Published online by Cambridge University Press

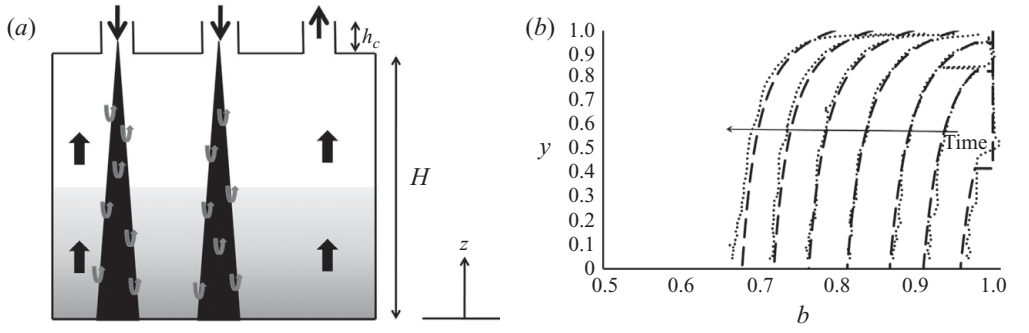


FIGURE 12. (*a*) Cartoon showing two plumes going in and one going out. (*b*) Comparison of experimental data (dotted line) and the theoretical prediction (dashed line) for experiments with three stacks. $h_c = 6\,\mathrm{cm}$; the initial salinity is 15 %.

(cf. (2.21*a*)–(2.21*d*)) with initial conditions

$$\int_0^1 \Delta_N(y)\,\mathrm{d}y = 1, \tag{5.6a}$$

$$q_n(1) = (\hat{\Gamma} P)^{5/3}/n, \tag{5.6b}$$

$$m_n(1) = \hat{\Gamma}^{10/3} P^{4/3}/n^2, \tag{5.6c}$$

$$f_n(1) = 1/n, \tag{5.6d}$$

$$f_n(0) = 0, \tag{5.6e}$$

where

$$\hat{\Gamma} = \left(\frac{F_{N0} d^5}{Q_{N0}^3}\right)^{-1/5}, \tag{5.7}$$

and F_{N0} and Q_{N0} are the total buoyancy flux and volume flux for all the stacks combined, respectively. The factors of n in the above equations arise in order that the total volume flux and buoyancy flux of all the n plumes coincide with those in (2.23) and (2.11) for the total volume flux, Q_N, and momentum flux, M_N, for a single inflowing plume. Since these equations are directly analogous to those of § 2, the model produces analogous solutions with the key difference being associated with the mixing produced by n plumes, which leads to a different value of ω for a given initial buoyancy flux.

We have tested the predictions of (5.5)–(5.7) with some further experiments for the particular case of $N = 3$. There are two possible flow regimes: (i) one incoming plume and two plumes leaving the space, i.e. $n = 1$, and (ii) there can be inflow through two stacks and outflow through the third, i.e. $n = 2$ (figure 12*a*). For these experiments, we modified our experimental set-up from § 3 by adding a third hole of the same diameter in the bottom of the tank in which we inserted a third stack of the same height as the other two. Whilst in the experiment the fact that both regimes are equally likely the specific flow regime that develops depends on the order in which the bungs are pulled out and any associated small perturbations to the flow. For one incoming plume, the theory is very similar to that discussed in previous sections and thus we concentrate on the case of two inflowing plumes. Figure 12(*b*) illustrates the short- and long-term evolution of the interior stratification when there are two

https://doi.org/10.1017/S0022112010005392 Published online by Cambridge University Press

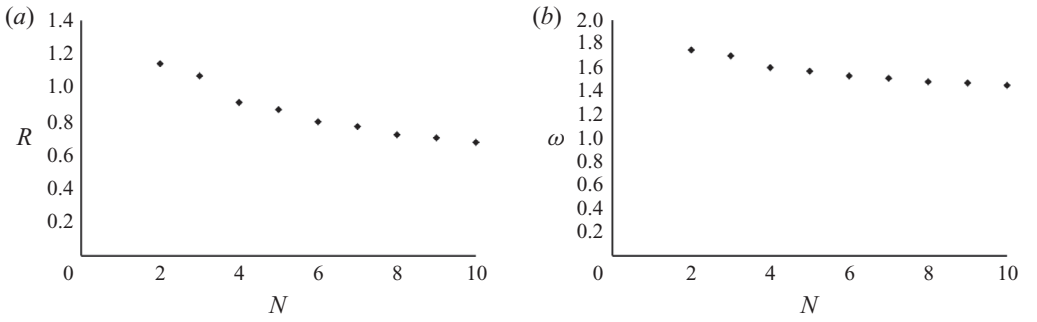


FIGURE 13. (*a*) $R=(b(1)-b(0))/\bar{b}$ as a function of N. (*b*) ω as a function of N. The variable n is the number of inflowing plumes to maximise the volume flux. $\hat{\Gamma}P=0.25$. For $N=2$, $\Gamma=1$.

incoming plumes as measured experimentally (dotted lines). These data are compared with the model prediction (dashed line). It can be seen that the experimental data match the theory very well.

In general, we can use the above model to explore the effect multiple stacks have on the mixing efficiency in the space. Figure 13(*a*) shows how the stratification, i.e. $R=(b(1)-b(0))/\bar{b}$, varies for multiple stacks with a constant volume flux, $\hat{\Gamma}P=0.25$. We consider the case where n, the number of inflowing plumes, is chosen to maximise the volume flux through the vents, i.e. for N even, $n=N/2$ and for N odd, $n=(N-1)/2$ (cf. figure 11). The figure illustrates that as the number of stacks increases, the degree of stratification in the interior, R, decreases rapidly and the space becomes more well mixed. As a result, the value of ω decreases as the number of stacks increases (figure 13*b*), and thus, the average density in the interior decreases more slowly.

6. Conclusion and applications

We have presented a model for the buoyancy-driven mixing of an enclosed fluid during draining, based on the theory of turbulent buoyant plumes. We have shown that the model admits separable solutions in time and space, and the model predictions are broadly consistent with some new experiments designed to explore this flow regime.

The new modelling and experiments have identified that (i) significant vertical density stratification may develop and this extends understanding of the flow regime beyond the earlier well-mixed model presented by Linden *et al.* (1990). In itself, development of such stratification may lead to constraints on the design of winter mixing ventilation schemes to ensure thermal comfort of the occupants at low level as well as modelling the evolution of the mean temperature within the space; and (ii) the new modelling to predict the rate of ascent of surfaces of constant density, and any associated contaminants, through the space provides insight into the time for flushing contaminants (e.g., smells) using mixing ventilation in a fashion analogous to models of contaminant transport during displacement ventilation (e.g., Bolster & Linden 2007). Recognition that such contaminant surfaces migrate through the space and do not simply become well-mixed may be key for assessing the nature of contaminant hazards in a space ventilated using mixing ventilation.

In order to illustrate some of these points in detail, we now consider the ventilation in a large theatre building with area 1500 m^2 and height 10 m with chimneys of effective area 10 m^2 and height 3 m.

https://doi.org/10.1017/S0022112010005392 Published online by Cambridge University Press

6.1. *Temperature regulation*

During a performance, the audience heat up the space. In the interval, most people then leave the room and the air can be freshened and cooled down. If the exterior is colder than the comfort temperature, it is advisable to use mixing ventilation, as opposed to displacement ventilation to achieve such cooling. Using our model, it is possible to predict by how much the interior cools in a given period of time. For example, if the density contrast with the exterior is 10–20 °C, it would take roughly 15–20 min to decrease the temperature by 50 % with the two stacks (cf. (2.4)). If this is not sufficient, one can consider opening a third chimney, thus increasing the volume flux (figure 11) and, with two incoming plumes, the mixing of the interior becomes more efficient.

We have also demonstrated that the interior stratification which develops during such a cooling event may be significant (figures 9 and 13*a*) and thus the temperature at the base of the atrium is noticeably colder than at the top. This may lead to overcooling at the base of the space if the ventilation persists for too long, even if the mean temperature is still acceptable. The control system should therefore monitor the temperature at the occupied level, and turn off the flow once that temperature reaches the minimum acceptable value.

6.2. *Flushing smoke and contaminants*

In the case of a fire in the theatre described above, it is important to understand how quickly the smoke leaves the space and also how the average concentration and the concentration of smoke in the occupied zone changes with time. The well-mixed model identifies that smoke with a temperature contrast of 100–150 °C would be reduced to 1/4, 1/9 and 1/16 of the initial concentration after times of τ, 2τ and 3τ. In a theatre with the given dimensions, this may range from about 37 to 47 min. Adding a third stack would increase the ventilation rate further and thus the smoke would be drained more quickly. Using (5.4), we can see that with just one more stack, the time scale to reduce the mean concentration to 3τ is decreased to the range 29–37 min. Similar to the analysis of the evolution of the mean concentration, our model of the stratification identifies that any high-concentration regions of smoke, rising from the source, will be carried up by the flow towards the exit vent over a transport time of order τ. If the source ceases to generate smoke, then beyond the time τ, the remaining smoke will be mixed by the plume through entrainment, and hence will become more dilute.

It is worth noting that if the external temperature is close to comfort conditions, then the ventilation regime should be changed to pure upward displacement ventilation (Linden *et al.* 1990; Gladstone & Woods 2001), since air can enter at low level and directly flow over the audience without the need for pre-heating (as is achieved with the mixing ventilation regime described above). In that case, the transient ventilation would lead to a deepening lower layer of air with temperature equal to the external temperature (cf. Fitzgerald & Woods 2007).

REFERENCES

Baines, W. & Turner, J. 1969 Turbulent buoyant convection from a source in a confined region. *J. Fluid Mech.* **37** (1), 51–80.

Bolster, D. T. & Linden, P. F. 2007 Contaminants in ventilated filling boxed. *J. Fluid Mech.* **591**, 97–116.

Bolster, D. T., Maillard, A. & Linden, P. 2008 The response of natural displacement ventilation to time-varying heat sources. *Energy Build.* **40**, 2099–2110.

https://doi.org/10.1017/S0022112010005392 Published online by Cambridge University Press

Boulard, T. & Baille, A. 1995 Modeling of air exchange rate in a greenhouse equipped with continuous roof vents. *J. Agric. Engng Res.* **61**, 37–48.

Bower, D. J., Caulfield, C. P., Fitzgerald, S. D. & Woods, A. W. 2008 Transient ventilation dynamics following a change in strength of a point source of heat. *J. Fluid Mech.* **614**, 15–37.

Caulfield, C. P. & Woods, A. W. 1998 Turbulent gravitational convection from a point source in a non-uniformly stratified environment. *J. Fluid Mech.* **360**, 229–248.

Caulfield, C. P. & Woods, A. W. 2002 The mixing in a room by a localized finite-mass-flux source of buoyancy. *J. Fluid Mech.* **471**, 33–50.

Chenvidyakarn, T. & Woods, A. W. 2005 Multiple steady states in stack ventilation. *Build. Environ.* **40**, 399–410.

Chiu, Y.-H. & Etheridge, D. W. 2004 Experimental technique to determine unsteady flow in natural ventilation stacks at model scale. *J. Wind Engng Ind. Aerodyn.* **92**, 291–313.

Fitzgerald, S. D. & Woods, A. W. 2007 On the transition from displacement to mixing ventilation with a localised heat source. *Build. Environ.* **42** (6), 2210–2217.

Fitzgerald, S. D. & Woods, A. W. 2008 The influence of stacks on flow patterns and stratification associated with natural ventilation. *Build. Environ.* **43**, 1719–1733.

Flynn, M. R. & Caulfield, C. P. 2006 Natural ventilation in interconnected chambers. *J. Fluid Mech.* **564**, 139–158.

Germeles, A. E. 1975 Forced plumes and mixing of liquids in tanks. *J. Fluid Mech.* **71**, 601–623.

Gladstone, L. & Woods, A. W. 2001 On buoyancy-driven natural ventilation of a room with a heated floor. *J. Fluid Mech.* **441**, 293–314.

Hunt, G. R. & Kaye, N. G. 2001 Virtual origin correction for lazy plumes. *J. Fluid Mech.* **435**, 377–396.

Kaye, N. G. & Hunt, G. R. 2004 Time-dependent flows in an emptying filling box. *J. Fluid Mech.* **520**, 135–156.

Kenton, A. G., Fitzgerald, S. & Woods, A. W. 2004 Theory and practice of natural ventilation in a theatre. *Proc. PLEA 2004*, Eindhoven.

Linden, P. 1999 The fluid mechanics of natural ventilation. *Annu. Rev. Fluid Mech.* **31**, 201–238.

Linden, P. F. & Cooper, P. 1996 Multiple sources of buoyancy in a naturally ventilated enclosure. *J. Fluid Mech.* **311**, 177–192.

Linden, P., Lane-Serff, G. & Smeed, D. 1990 Emptying filling boxes: the fluid mechanics of natural ventilation. *J. Fluid Mech.* **212**, 309–335.

Liu, P.-C., Lin, H.-T. & Chou, J.-H. 2009 Evaluation of buoyancy-driven ventilation in atrium buildings using computational fluid dynamics and reduced-scale air model. *Build. Environ.* **44**, 1970–1979.

Livermore, B. & Woods, A. W. 2006 Natural ventilation of multiple storey buildings: the use of stacks for secondary ventilation. *Build. Environ.* **41** (10), 1339–1351.

Merci, B. & Maele, K. V. 2008 Numerical simulations of full-scale enclosure fires in a small compartment with natural roof ventilation. *Fire Saf. J.* **43**, 495–511.

Morton, B., Taylor, G. & Turner, J. 1956 Turbulent gravitational convection from maintained and instantaneous sources. *Proc. R. Soc. Lond. Ser.* A **234** (1196), 1–23.

Pawlak, G. & Armi, L. 2000 Mixing and entrainment in developing stratified currents. *J. Fluid Mech.* **424**, 45–73.

Turner, J. S. 1979 *Buoyancy Effects in Fluids*. Cambridge University Press.

Wells, M. G. & Wettlaufer, J. S. 2007 The long-term circulation driven by density currents in a two-layer stratified basin. *J. Fluid Mech.* **572**, 37–58.

Woods, A. W., Fitzgerald, S. D. & Livermore, S. 2009 A comparison of winter preheating requirements for natural displacement and natural mixing ventilation. *Energy Build.* **41** (12), 1306–1312.

https://doi.org/10.1017/S0022112010005392 Published online by Cambridge University Press